22 Fluorescence-Lifetime Imaging Microscopy

Fluorescence microscopy is one of the most widely used tools in the biological sciences. There has been a rapid growth in the use of microscopy due to advances in several technologies, including probe chemistry, confocal optics, multiphoton excitation, detectors, computers, and genetically expressed fluorophores such as GFP. Perhaps the most limiting aspect of fluorescence microscopy is knowledge of the local probe concentrations within the cell. These concentrations are usually variable based on the affinity of the fluorophore for various biomolecules within the cell. For example, probes such as DAPI and Hoechst have affinity for nucleic acids and are primarily nuclear stains. Probes such as rhodamine 123 have affinity for mitochondria. The known affinities of probes for specific biomolecules is a basic tool of optical microscopy, histology, and fluorescence microscopy. However, in general, the concentrations of the probes in each region of the cell are not known.

In the 1980s the use of fluorescence microscopy expanded from staining biomolecules within cells to studies of the intracellular concentrations of ions and to detection of association of reactions within the cells. This emphasis on intracellular physiology required different types of fluorophores, ones which changed their spectral properties in response to the ion or in response to the binding reaction of interest. The best-known examples of such probes are the wavelength-ratiometric probes for cell calcium (Chapter 19). Wavelength-ratiometric probes were needed because the local concentrations of fluorophores within cells are not known. These concentrations are unknown because the probes diffuse rapidly, undergo photobleaching, and can be washed out of the cells. Also, the quantum yields of probes can change due to the local environment. Even if the local intensity of a fluorophore is measured it is difficult to use the intensity to determine the local concentration. Without knowledge of the probe concentration it is not possible to make quantitative use of intensity measurements within the cells.

Wavelength-ratiometric probes provide a way to make measurements that are independent of the local probe concentrations. Suppose the emission spectrum of a fluorophore changes in response to calcium. The ratio of the emission intensities at two wavelengths will depend on the calcium concentration, but the ratio will be independent of the probe concentration. This ratiometric measurement allows quantitative information to be obtained from the images without precise knowledge of the probe concentrations in each region of the cell.

Fluorescence-lifetime imaging microscopy (FLIM) provides measurements that are independent of probe concentration. The intensity of a fluorophore depends on its concentration. However, the lifetime of a fluorophore is mostly independent of its concentration. Suppose the lifetime of a probe changes in response to pH, calcium, or some other analyte. If the lifetime is measured this value can be used to determine the analyte concentration, and the determination will be independent of the probe concentration.

The concept of fluorescence-lifetime imaging is illustrated in Figure 22.1. Suppose that the cell has two regions, each with an equal steady-state fluorescence intensity. Assume further that the lifetime of the probe in the central region of the cell (τ_2) is several-fold longer than that in the outer region (τ_1). The longer lifetime in the central region could be due to the presence of an ionic species such as calcium, binding of the probe to a macromolecule, or other environmental factors. The quantum yields of the probe in the central and outer regions could be the same or different due to interactions of the probe with biomolecules. The concentrations of the probe could be different due to partial exclusion of the probe from some region of the cell. The intensity image will not reveal the different environments in regions 1 and 2 (lower left). However, if the lifetimes were measured in regions 1 and 2 then the distinct environments would be detected. FLIM allows image contrast to be based

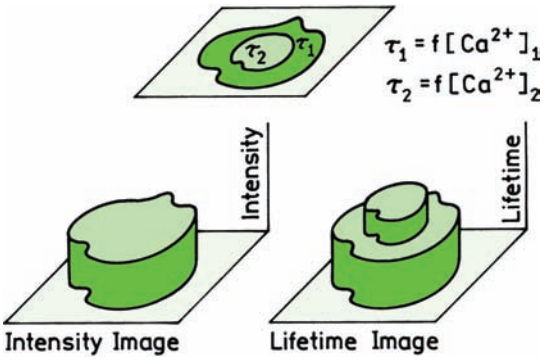

Figure 22.1. Intuitive presentation of the concept of fluorescence-lifetime imaging (FLIM). The object is assumed to have two regions that display the same fluorescence intensity but different decay times, $\tau_2 > \tau_1$.

on the lifetimes in each region of the cell, which can be presented on a color scale or as a 3D surface in which the height represents the local decay times.

The concept of FLIM is an optical analogue of magnetic resonance imaging (MRI). In MRI the proton relaxation times at each location in the patient are measured. The numerical value of the relaxation time is used to determine the contrast in the calculated image. The MRI images are presented as grayscale images because they are familiar to radiologists. The local chemical composition of the tissue determines the proton relaxation times. MIR image contrast is not based on signal intensity or proton concentration. The contrast in FLIM is determined by similar principles. The local environment determines the fluorescent lifetime, which is then used to calculate an image that is independent of probe concentration.

It is more difficult to measure lifetimes than intensities. So what is the value of FLIM? The advantages of lifetime imaging frequently justify the effort. There are a relatively small number of wavelength-ratiometric probes useful for intracellular use. Most of the available wavelength-ratiometric probes are for the divalent ions calcium and magnesium. There are fewer wavelength-ratiometric probes for the monovalent ions sodium and potassium, and these probes are more difficult to use. The wavelength-ratiometric probes for sodium absorb in the UV and display only small spectral changes. There are a larger number of probes that display changes in lifetime in response to ions or the environment, without displaying spectra shifts. For example, there are several long-wavelength probes for sodium that change intensity but not wavelength (Chapter 19). Probes for chloride are based on collisional quenching, which decreases the lifetimes but does not cause a spectral shift. In general, there are more lifetime probes for ions than there are wavelength-ratiometric probes.

Another advantage of lifetime imaging is that intracellular measurements of FRET using the donor lifetimes can be more reliable than intensity measurements of the donor and/or acceptor. Suppose the cell contains two proteins that associate with each other in response to a stimulus, and that the proteins are labeled each with a donor or acceptor. In principle the extent of association can be determined from the decrease in donor intensity. However, since the local donor concentration is not known the extent of quenching cannot be determined from the donor intensity alone. The intensity of the donor in the absence of acceptor must also be known. Such control measurements are difficult to perform when using cells. Why not use the donor-to-acceptor intensity ratio? This ratio is difficult to use because the local acceptor concentration is also unknown and the donor and acceptor labeled proteins may not be present at equal concentrations within the cell. The intensity ratio can be different due to different donor and acceptor concentrations as well as differences in the RET efficiency. Determination of the extent of binding is more straightforward using the donor lifetime. The donor lifetime will be decreased by FRET to a bound acceptor. The donor lifetime will not be affected by an acceptor-labeled protein that is not bound to the donor-labeled protein. If the donor intensity is well above the background intensity the donor lifetime will be independent of its concentration.

Creation of a lifetime image with reasonable spatial resolution requires measurement of 256 x 256 or more individual lifetime measurements, or even more lifetimes if higher spatial resolution is required. Additionally, the lifetimes have to be measured using a microscope. There are two general approaches to FLIM. The FLIM images can be measured using scanning methods when the lifetime is measured at discrete locations. Lifetime images can also be measured by wide-field methods even in solution when a time-resolved imaging detector is used. Because of the difficulty of measuring a single lifetime the concept of lifetime imaging seemed impractical with the technology available in the 1980s and early 1990s. Even if such measurements could be performed, the data acquisition times would be excessively long, precluding studies of live cells. At present the situation is completely different. Because of advances in technology FLIM studies of cells are now practical, and are becoming almost routine. FLIM can be performed using time-domain or frequency-domain methods, and by variants

of these methods, and the use of FLIM is increasing in the biosciences.

22.1. EARLY METHODS FOR FLUORESCENCE-LIFETIME IMAGING

In Chapter 4 we mentioned that the first lifetimes were measured by the phase method. Similarly, the first lifetime images were obtained using a phase method. In the late 1980s it was not practical to create a lifetime image using pixel scanning, and a wide-field method was needed. CCD cameras were available for wide-field steady-state imaging. However, CCDs are slow accumulating detectors which do not provide an opportunity for the nanosecond time resolution needed for FLIM. This problem was solved by using a gain-modulated image intensifier as an optical phase-sensitive detector.[1–4]

In Section 5.12 we described phase-sensitive detection. The phase angle of the detector is set at a known value relative to the phase of the incident light and the phase-sensitive intensity is measured. The phase-sensitive intensity is a steady-state signal that is proportional to $\cos(\theta - \theta_D)$ where θ_D is the phase angle of the detector and θ is the phase angle of the emission. If the phase-sensitive intensity is measured using several detector phase angles then the phase angle or lifetime of the emission can be determined. Phase-sensitive detection can be used to measure lifetime images using an image intensifier instead of a PMT (Figure 22.2). In this figure the sample consists of four cuvettes, each containing a fluorophore with a different lifetime or a calcium-sensitive fluorophore. These cuvettes are illuminated with the same laser beam. The phase and modulation of the emission from each cuvette is different due to the different decay times.

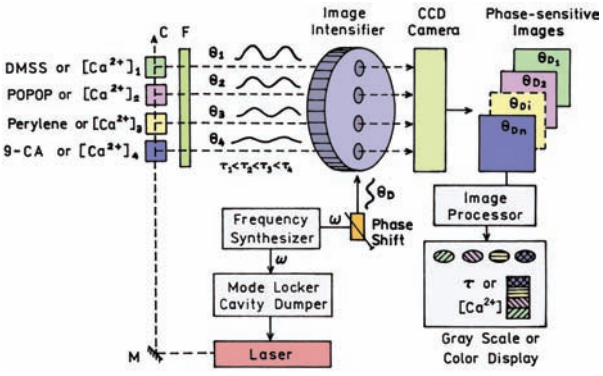

Figure 22.2. Schematic diagram of an FLIM experiment. The "object" consists of a row of four cuvettes each with a different fluorophore or a calcium-sensitive fluorophore with different calcium concentrations. The lifetime of the four samples are different. These cuvettes are illuminated with intensity-modulated light. The emission is detected with a phase-sensitive image intensifier, which is imaged onto a CCD camera. The light source is a pulsed laser.

Lifetime imaging was accomplished by measuring the images using a frequency-modulated image intensifier. The gain or voltage across the intensifier is modulated at the same frequency as the frequency of the modulated excitation, and the signals are phase locked so there is no drift between them. This measurement results in a constant image where the intensity at each location in the image is proportional to $\cos(\theta(r) - \theta_D)$ where $\theta(r)$ is the phase angle of the emission at position r. The image intensifier contains a phosphor screen where the brightness is proportional to the intensity, and the intensity is recorded with a CCD camera. The result is a steady signal from each cuvette, which is the phase-sensitive intensity. This configuration results in an optical phase-sensitive detector operating at the same frequency as the light modulation. This approach is analogous to using a PMT as a high-frequency phase-sensitive detection.[5]

Measurement of a single phase-sensitive intensity is not adequate to determine the lifetime. The phase angle and modulation of the emission can be determined by collection of a series of phase-sensitive images using different detector phase angles. At any position in the sample the phase-sensitive intensity is given by

$$I(\theta_D,r) = kC(r)\left(1 + \frac{1}{2}m_D m(r)\cos\{\theta(r) - \theta_D\}\right) \quad (22.1)$$

In this expression m_D is the modulation of the detector, $m(r)$ is the modulation of the emission at position r, k is a constant, and $C(r)$ is the concentration or steady-state intensity of the fluorophore at position r. The detector is in phase with a zero lifetime when the detector angle $\theta_D = 0$.

Measurement of lifetimes from the phase-sensitive intensities is illustrated in Figure 22.3. The cell is illuminated with light modulated at 80 MHz. The phase angle and modulation of the emission is different in these two regions because of the different lifetimes. The phase-sensitive intensities and modulations are different in each region of the cell due to the different lifetimes. The phase angles and modulations in each region are determined by fitting the phase-sensitive intensities to a cosine function. The phase angle or modulation image is then used to calculate the lifetime image.

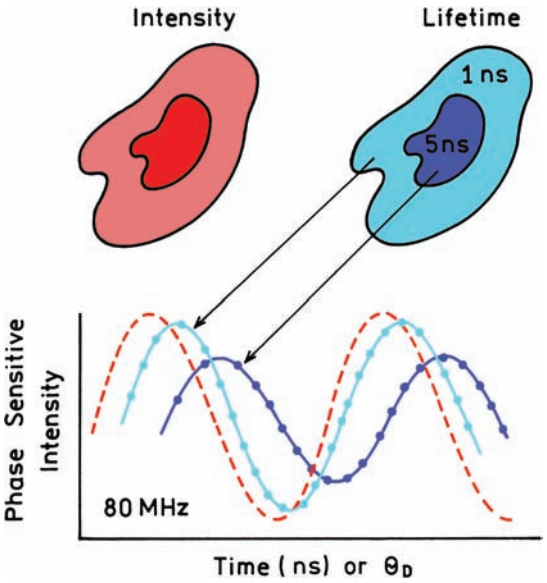

Figure 22.3. Schematic of lifetime imaging using phase-sensitive images.

22.1.1. FLIM Using Known Fluorophores

The actual use of phase-sensitive images to measure lifetime images is shown in Figure 22.4. The excitation is passed through four cuvettes, each containing a fluorophore with a different lifetime. DMSS has the shortest lifetime, smallest phase angle, and highest modulation. 9-Cyanoanthracene has the longest lifetime, largest phase angle, and smallest modulation. The phase-sensitive intensities at the various detector phase angles can be fit to determine the phase angle and modulation of the emission. Since the phase-sensitive intensities were measured using an imaging detector, the data can be used to create an image when the contrast or color is based on phase angle, modulation or apparent lifetime.

22.2. LIFETIME IMAGING OF CALCIUM USING QUIN-2

22.2.1. Determination of Calcium Concentration from Lifetime

Lifetime imaging depends on the use of a probe that changes lifetime in response to a change in conditions. Imaging of calcium concentrations requires a probe that displays calcium-dependent lifetimes. Figure 22.5 shows non-imaging frequency-domain data for the calcium probe Quin-2 with various concentrations of calcium.[6] The frequency response shifts dramatically to lower frequencies at

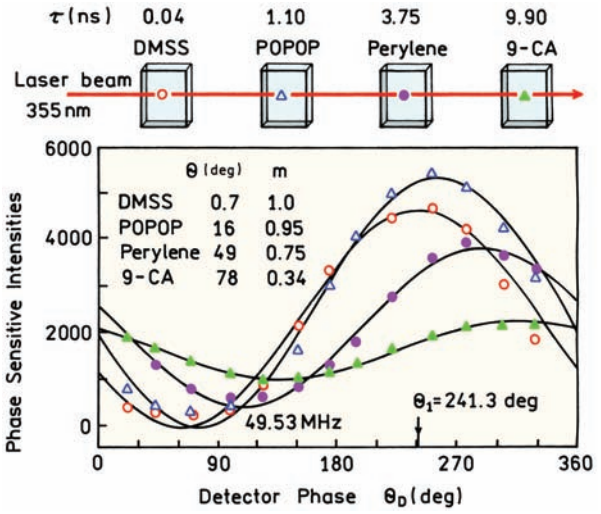

Figure 22.4. Phase-sensitive intensities of standard fluorophores at various detector phase angles. The decay times from left to right are 0.04 (○), 1.10 (Δ), 3.75 (●), and 9.90 ns (▲). The modulation frequency was 49.53 MHz. DMSS, 4-dimethylamino-ω-methylsulfonyl-*trans*-styrene; 9-CA, 9-cyanoanthracene; POPOP, *p*-bis[2-(5-phenyloxazazolyl)]benzene. θ_1 is the arbitrary phase angle of the incident light.

higher concentrations of calcium. At intermediate calcium concentrations near 8 nM the decays are multi-exponential, as can be seen from the shape of the frequency response. The data were fit globally to two lifetimes: $\tau_1 = 1.38$ ns and $\tau_2 = 11.58$ ns, with amplitudes that depend on the calcium concentration.

The data in Figure 22.5 can be used to create a calibration curve for calcium (Figure 22.6). These curves can be used to determine the concentration of calcium from the phase or modulation of the emission. It is important to rec-

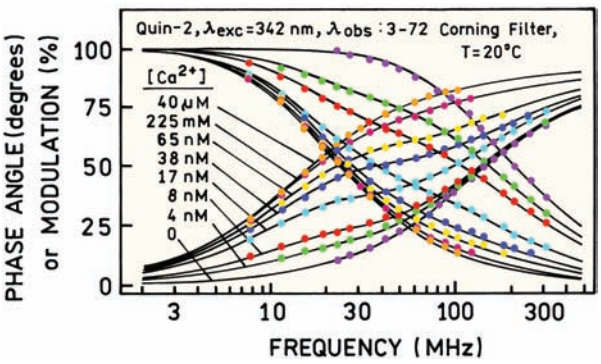

Figure 22.5. Frequency-domain intensity decays for Quin-2 with varying concentrations of calcium. The data were fit globally with two lifetimes $\tau_1 = 1.38$ ns and $\tau_2 = 11.58$ ns.

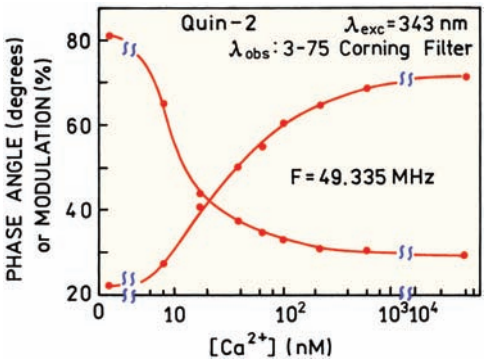

Figure 22.6. Dependence of the phase angle and modulation of Quin-2 on the calcium concentration. Revised from [7].

ognize that the calcium concentrations can be determined using measurements at a single modulation frequency without resolution of the multi-exponential decay. This is because there is always a single phase angle and modulation of the emission irrespective of the complexity of the decay. Of course, a different calibration curve would be obtained using different modulation frequencies.

22.2.2. Lifetime Images of Cos Cells

Once a calibration curve is known the phase and modulation values can be used to determine calcium concentrations in cells. Fluorescence intensity images for Quin-2 in three Cos cells are shown in Figure 22.7. The intensity of Quin-2 is highly variable in different regions of the cells (top). The intensity images alone do not indicate if the intensity differences are due to differences in Quin-2 concentrations or to different calcium concentrations. Phase-sensitive images were obtained using the apparatus shown in Figure 22.2 and the phase angles determined at each location in the image. In contrast to the intensities the phase angles are more constant throughout the cells (Figure 22.7, middle). The phase angle image can be converted to a calcium concentration image (bottom) using a calibration curve like that in Figure 22.6. The calcium concentration appears higher in the periphery of the cells than near the center. The regions of lower calcium concentration correspond to regions of lower phase angles. The calcium concentration images are more constant than are the intensity images. This result indicates that most of the intensity variations seen in Figure 22.7 are due to differences in Quin-2 concentrations rather than locally different calcium concentrations. The use of FLIM allowed the calcium concentrations to be determined with-

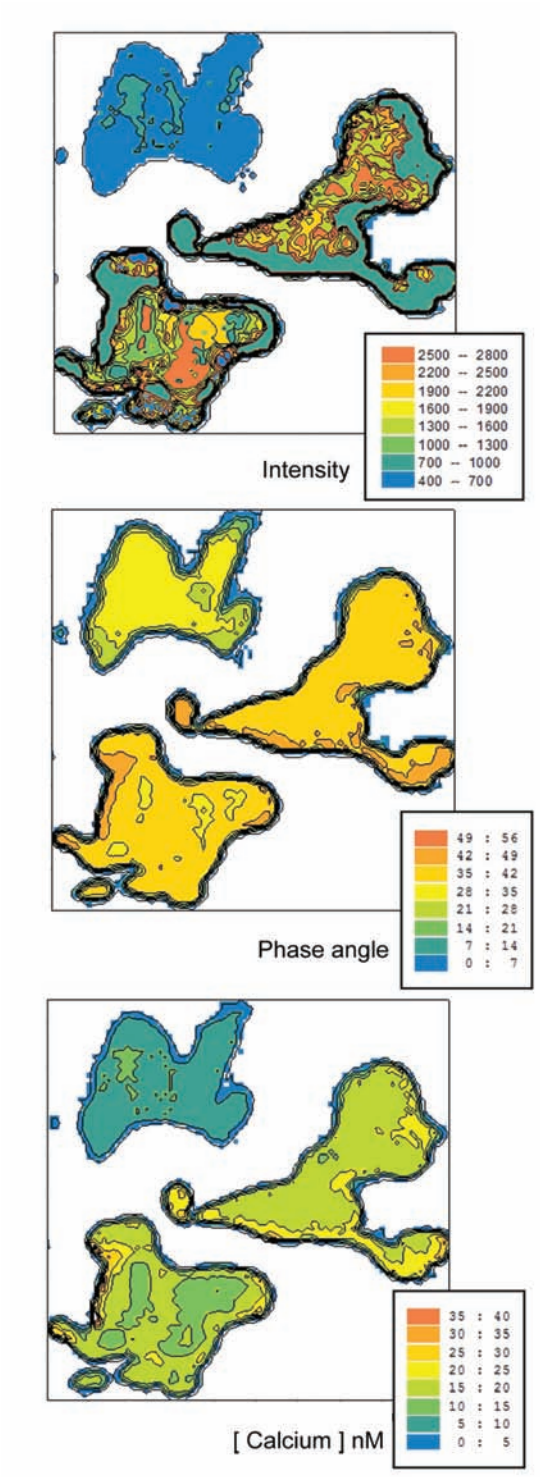

Figure 22.7. Fluorescence imaging of Cos cells labeled with Quin-2. Top, intensity. Middle, phase angle image at 45.53 MHz. Bottom, calcium concentration image. The calibration curve used to calculate the calcium concentration is different from Figure 22.6, and included a photobleaching correction. Reprinted with permission from [7].

out knowledge of the local probe concentrations within the cell.

22.3. EXAMPLES OF WIDE-FIELD FREQUENCY-DOMAIN FLIM

Since the early use of FLIM for calcium imaging there has been a dramatic increase in the use of FLIM.[8–13] Several methods can be used to create lifetime images, including time-domain, frequency-domain, and gated methods. A number of laboratories have constructed wide-field frequency-domain FLIM instruments.[14–19] Additional references on FLIM methods and applications are listed in the section entitled Additional Reading on Fluorescence-Lifetime Imaging Microscopy near the end of the chapter.

22.3.1. Resonance Energy-Transfer FLIM of Protein Kinase C Activation

Wide-field frequency-domain FLIM can be used to study the activation of intracellular proteins. One example is the use of FLIM to study protein phosphorylation in response to stimuli.[20–22] Figure 22.8 shows images of Cos7 cells that expressed GFP-labeled protein kinase C (PKC). The intensity images in the top panels show the locations of GFP-labeled PKC. This protein is phosphorylated upon activation by the tumor-producing substance phorbol myristoyl acetate (PMA). The cells were microinjected with Cy3.5-labeled IgG that is specific for the phosphorylated epitope of PKC. Binding of the labeled antibody to PKC is expected to reduce the lifetime of the GFP label by resonance energy transfer to the acceptor Cy3.5.

The lower panels in Figure 22.8 show the lifetime images of the three cells at various times. Initially the GFP lifetimes are the same in all the cells and constant within the cells. At later times the GFP lifetime in the central cell decreases. All the cells were treated with PMA, and only the central cell was injected with Cy3.5-labeled IgG specific for phosphorylated PKC. The lifetime of GFP-PKC in the central cell decreases because of energy transfer to the Cy 3.5-labeled antibody. These images are not confocal so it is difficult to know if phosphorylated PKC appears uniformly throughout the cell or is localized near the membrane.

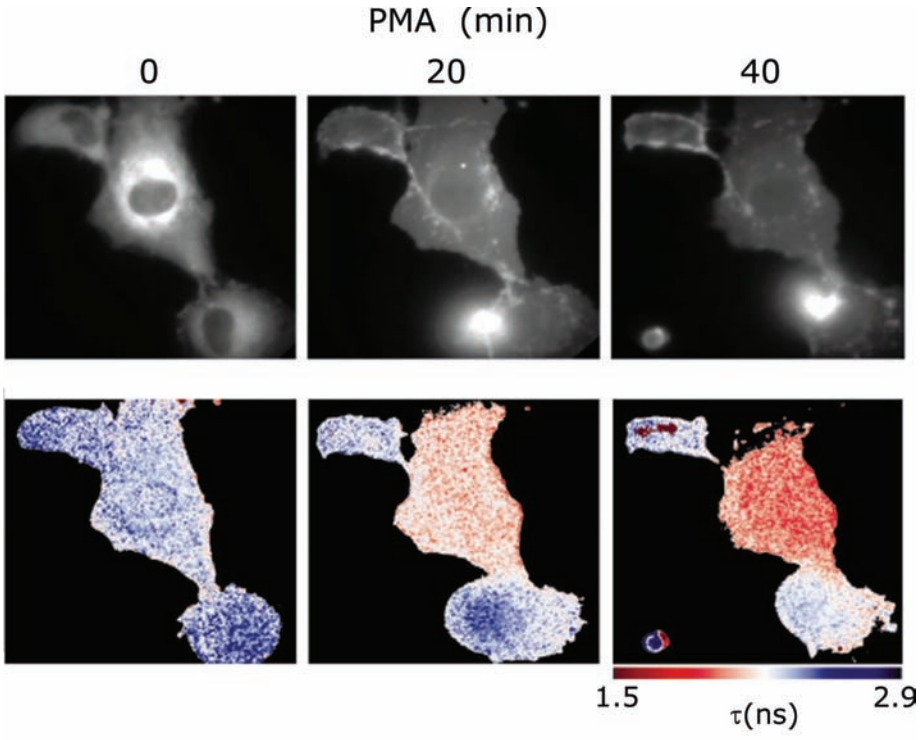

Figure 22.8. Activation of lipid/calcium-dependent protein kinase C (PKC) in Cos7 cells. The top panels show the intensity images of GFP-tagged PKC. All the cells were treated with phorbol myristoyl acetate (PMA). The lower panels show the GFP-lifetime images the central cell was injected with Cy3.5-IgG specific for the phosphorylated epitope of PKC. Reprinted with permission from [22].

The images in Figure 22.8 show an advantage of using lifetime images as compared to intensity images. In principle RET from GFP to Cy3.5 could have been measured using intensity ratios of GFP to Cy 3.5. However, the ratios would not allow the extent of RET to be calculated without knowledge of the local concentrations of unbound acceptor. The donor lifetime is not affected by unbound acceptor and thus reflects the extent of acceptor binding to GFP-PKC and the extent of its phosphorylation. The donor-to-acceptor intensity ratio would be dependent on the concentration of unbound acceptor.

22.3.2. Lifetime Imaging of Cells Containing Two GFPs

GFP-labeled proteins are widely used in cellular imaging. Because of the need to monitor more than a single intracellular protein a number of GFP mutants have been developed with different absorption and emission wavelengths. However, the wide absorption and emission spectra of the GFPs limit the number that can be observed in a single experiment. One approach to distinguishing more GFPs is to use lifetimes instead of or in addition to wavelength to identify the GFP.[23]

The possibility of resolving multiple GFPs using lifetimes is shown in Figure 22.9. These panels show Vero cells that are expressing more than one type of GFP. All the cells express YFP5 in the cytoplasm that displays a lifetime near 3.4 ns. The cells also express GFP5 that displays a lifetime near 2.2 ns. In the upper left GFP5 is located near the golgi. In the other three cells GFP5 is localized in the nucleus. The presence and location of GFP5 can be seen as a decrease in lifetime in these regions of the cell. This effect is most obvious for the cell in case YFP5 was not present in the nucleus (lower right), so that the emission is mostly due to GFP5, which has a shorter lifetime. These results show how FLIM can be used to resolved similar molecules in cells if the lifetimes are different.

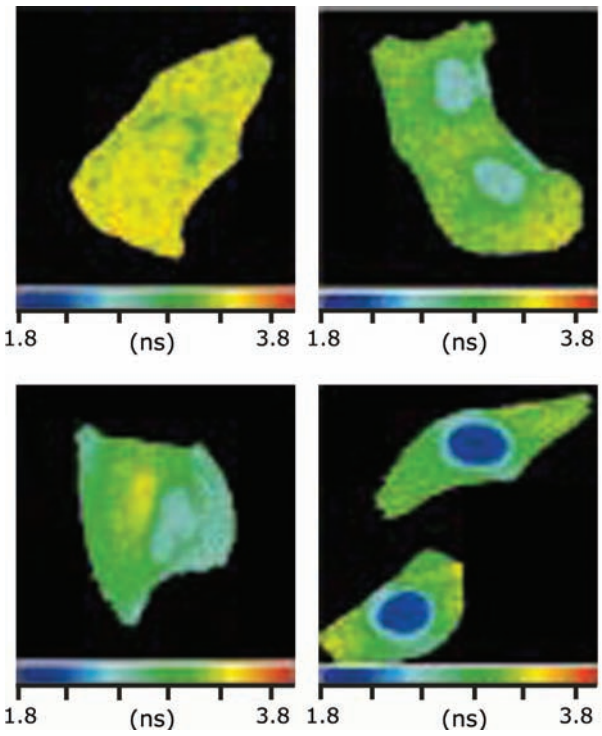

Figure 22.9. Lifetime images of Vero cells expressing two GFPs. All cells express YFP5 ($\tau = 3.4$ ns) in the cytoplasm. The cells in the upper right and lower left express GFP5 localized in the nucleus. The cell in the lower right does not have YFP5 in the nucleus so that only the shorter lifetime GFP5 contributes to the signal. Reprinted with permission from [23].

22.4. WIDE-FIELD FLIM USING A GATED-IMAGE INTENSIFIER

Another approach to lifetime imaging is analogous to the pulse sampling method described in Section 4.8.1. Instead of sinusoidally modulating the gain of the image intensifier, the intensifier is gated on for short periods of time (Figure 22.10). The intensity images collected at various time delays are used to calculate the lifetime at each pixel.[24–35] The time intervals can be non-overlapping, as shown in Figure 22.10, or overlapping to provide a larger signal in each image. Gated-image intensifiers are commercially available

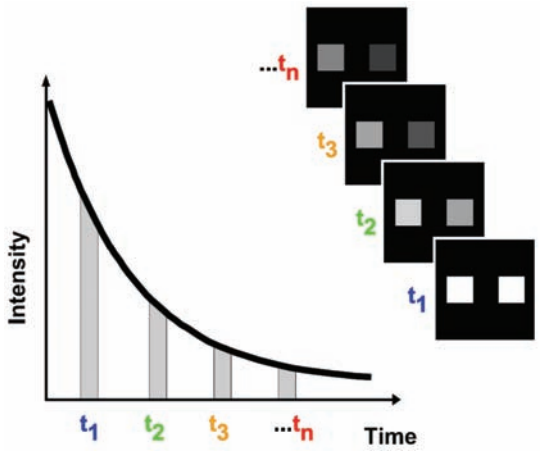

Figure 22.10. Schematic of FLIM using a gated-image intensifier. Reprinted with permission from [35].

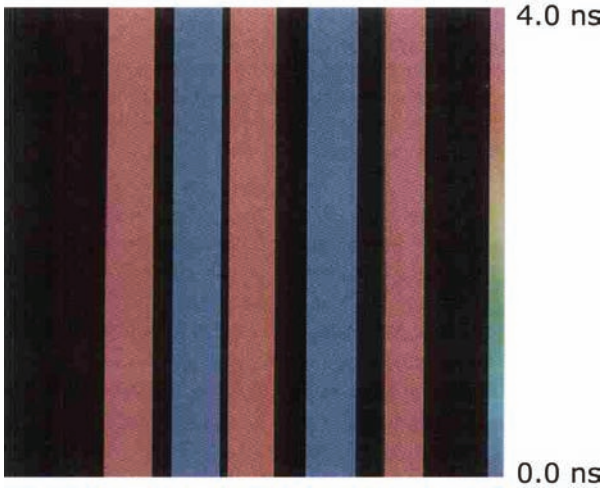

Figure 22.11. FLIM of small containers of Coumarin-314 (τ = 3.46 ns) and 2-(p-dimethylamino-styryl)-pyridylmethyl iodide (DASPI, τ = 143 ps) in a 50:50 mixture of water and glycerol. Reprinted with permission from [35].

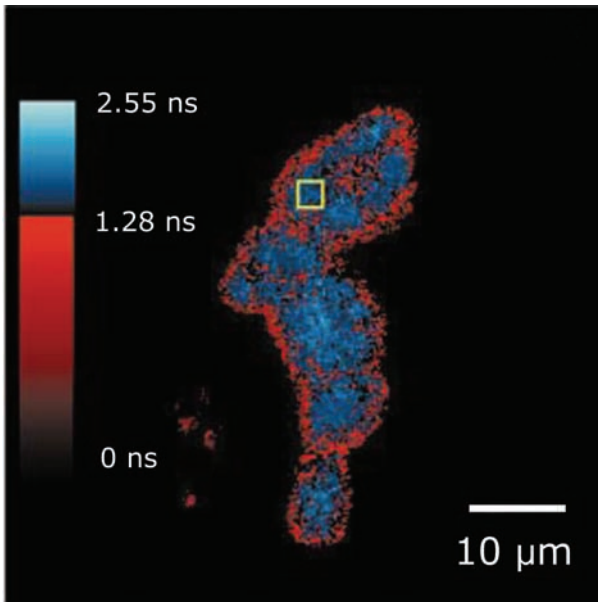

Figure 22.12. FLIM of small containers of Coumarin-314 (τ = 3.46 ns) and 2-(p-dimethylamino-styryl)-pyridylmethyl iodide (DASPI, τ = 143 ps) in a 50:50 mixture of water and glycerol. Reprinted with permission from [35].

and in the past several years have become fast enough for nanosecond FLIM.[36–38]

The lifetime images obtained using a gated-image intensifier can be relatively free of noise. Figure 22.11 shows lifetime images of small samples of Coumarin-314 (τ = 3.46 ns) and of DASPI (τ = 143 ps). The images clearly distinguish the two lifetimes, and the lifetime is constant in each solution. FLIM with a gated intensifier has also been applied to cellular imaging. In this case the time windows for gating were 2 ns wide and spaced 1 ns apart.[28] The gated time intervals were overlapped in time. Figure 22.12 shows lifetime images of protein dimerization in mouse pituitary cells. These cells expressed the transcription factor EBPΔ224, which was fused with GFP. Two fusion proteins of this transcription factor were expressed, one with CFP and another with YFP, which served as a donor–acceptor pair. The presence of dimers of EBPΔ224 is seen around the periphery of the cell as a decreased lifetime for the donor.

22.5. LASER SCANNING TCSPC FLIM

An alternative to wide-field microscopy is laser scanning microscopy (LSM). When using LSM the images are created by sequentially measuring all the pixels in an image.[39] This is accomplished by scanning a focused laser beam across the sample and measuring the intensities at each position. LSM is usually performed using confocal optics to reject out-of-focus fluorescence. LSM is also performed using multiphoton excitation, in which case out-of-plane fluorescence is not excited and the confocal pinholes are not needed. LSM offers many opportunities for lifetime imaging because of the well-developed technology for time-resolved measurements using point detectors such as PMTs and APDs.

Figure 22.13 shows a schematic for TCSPC when using a laser scanning microscope. The basic idea is to perform the TCSPC measurements while the laser scans across the sample. At each point in the image the instrument measures a decay curve. This is possible because the repetition rate of the laser is usually high enough that many excitation pulses arrive during the dwell time at each pixel. For example, if the dwell time is 20 µs and the laser repetition rate is 80 MHz, then 1600 pulses arrive at each pixel while scanning a single image. The data are then stored in a three-dimensional matrix. The *x*- and *y*-axes indicate the position in the sample (Figure 12.13). The third dimension represents the arrival times of the photons associated with each pixel in the image.

The principle of TCSPC FLIM is straightforward but its implementation is complex.[41–52] Specialized hardware and software is needed to keep track of the time between the laser pulses and detected photons, and the position of the laser beam on the sample. Fortunately, these capabilities are

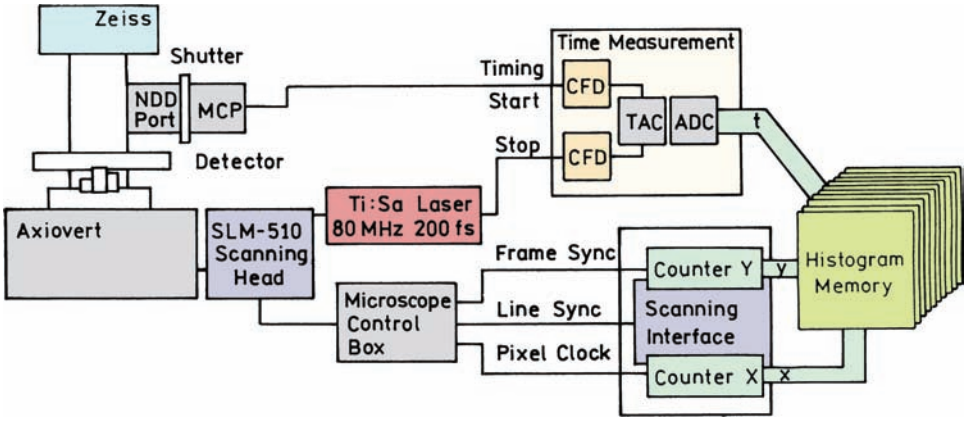

Figure 22.13. Schematic for FLIM using TCSPC. Revised from [40].

available commercially and can be added to laser scanning microscopes. TCSPC appears to have many advantages for FLIM. Since individual photons are counted the measurements provide high efficiency. TCSPC makes use of all the photons reaching the detector. FLIM using a gated-image intensifier only makes use of a small fraction of the photons that arrive while the gate is open. Frequency-domain FLIM uses more of the available photons than gating, but the duty cycle is 50% or less. Using all the available photons is an important feature in fluorescence microscopy because the fluorophores are being photobleached during observation.

The total time to acquire a lifetime image depends on the photon count rate and the desired accuracy in the decay times. A single-exponential lifetime can be estimated with 10% accuracy with 185 photons.[51] At a count rate of 10^6 photons/s acquisition of 200 photons requires 0.2 ms and data for a 128 x 128 lifetime image can be acquired in 3.3 s. It is easily possible to collect 200 photons with a dwell time of 0.2 ms because there will be 16,000 excitation pulses. The time needed to acquire an FLIM image increases dramatically if it is necessary to resolve a double exponential decay at each pixel. Resolution of a double-exponential decay to an accuracy of 10% requires 10,000 to 100,000 photons.[51] Hence the time to acquire the data can become longer than practical with biological samples.

Presently available technology for TCSPC imaging goes beyond that shown in Figure 22.14. Many laser scanning microscopes have multiple detectors for emission at different wavelengths. Multiple detectors are useful because cells are often labeled with more than one fluo-

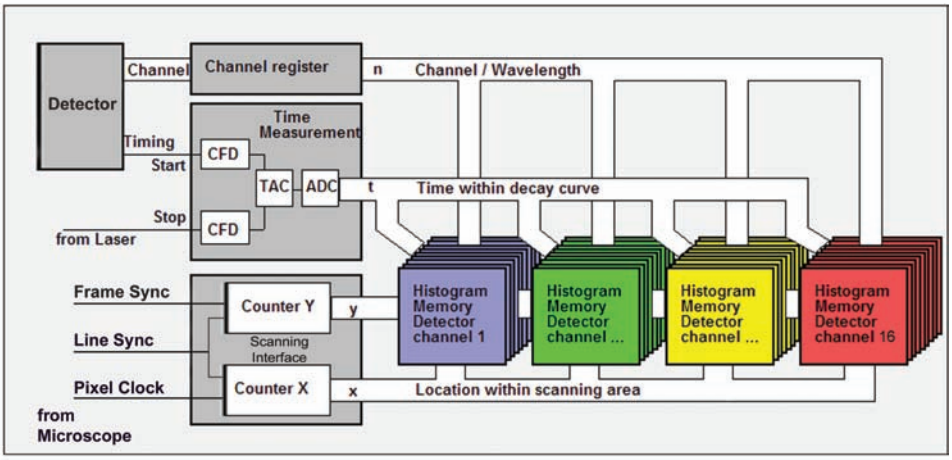

Figure 22.14. Schematic for multi-wavelength TCSPC lifetime imaging. Reprinted with permission from [49].

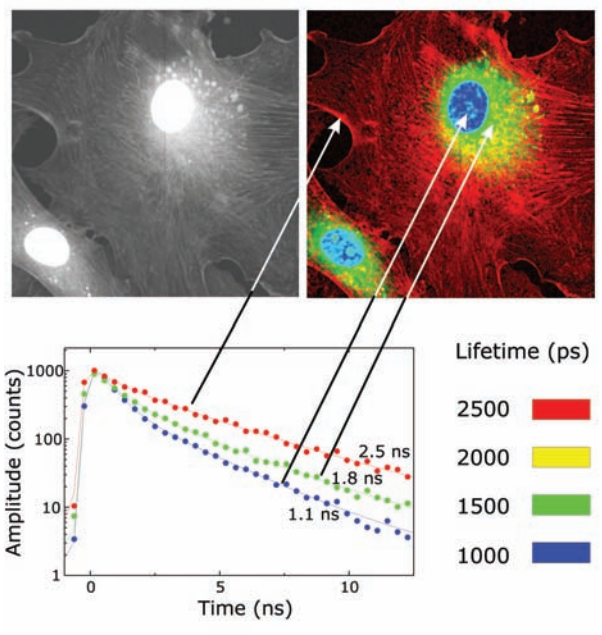

Figure 22.15. Intensity (left) and lifetime image (right) of bovine artery endothelial cells. The nuclei were stained with DAPI for DNA (blue), F-actin was stained with Bodipy FL-phallacidin (red), and the mitochondria were stained with MitoTracker Red CMX Ros (green). Two-photon excitation of 800 nm. Courtesy of Dr. Axel Bergman, Becker & Hickl GmbH.

rophores, some ion indicators are wavelength-ratiometric, and donor and acceptor intensities can be measured simultaneously.

22.5.1. Lifetime Imaging of Cellular Biomolecules

FLIM can yield dramatic images showing the locations of different biomolecules within cells. Figure 22.15 shows intensity and lifetime images of bovine artery endothelial cells stained with three fluorophores. Nucleic acids were stained with DAPI, F-actin was stained with Bodipy FL-phallacidin, and the mitochondria were stained with MitoTracker Red CMX Ros. The intensity image shows regions of the cell with different brightness but does not distinguish between the three fluorophores. TCSPC measurements in each region of the cell showed that DAPI decayed with a lifetime of 1.1 ns, Bodipy-FL displayed a lifetime of 2.5 ns, and MitoTracker CMX Ros displayed a lifetime of 1.8 ns. These lifetimes were used to assign pseudocolors to each of the fluorophores. The lifetime image clearly resolved the locations of the probes based on their lifetimes.

22.5.2. Lifetime Images of Amyloid Plaques

Alzheimer's disease is associated with the accumulation of plaques composed primarily of an amyloid peptide that forms β-sheets. Formation of the plaques depends on the presence of presenilin 1 (PS1), which contains part of the enzymatic activity needed for plaque formation. Lifetime imaging was used to determine the location of PS1 in Chinese hamster ovary (CHO) cells that expressed this protein. The cells were stained with fluorescein-labeled antibodies that bound closely to PS1. The lifetime of these antibodies was mostly constant throughout the cell (Figure 22.16). The cells were then exposed to Cy3-labeled antibodies that also bound closely to PS1 and serve as an acceptor for FITC. The presence of the Cy3 acceptor resulted in a decrease in the lifetime of the FITC donor.[53] The mean lifetime of FITC changed from about 2.6 ns in the absence of acceptor to about 1.6 ns in the presence of acceptor. These results show that RET and laser scanning FLIM can be used to detect local proximity of proteins within cells.

22.6. FREQUENCY-DOMAIN LASER SCANNING MICROSCOPY

Laser scanning microscopy can also be used with frequency-domain measurements for lifetime imaging.[54–57] The instrumentation is similar to that shown in Figure 22.13

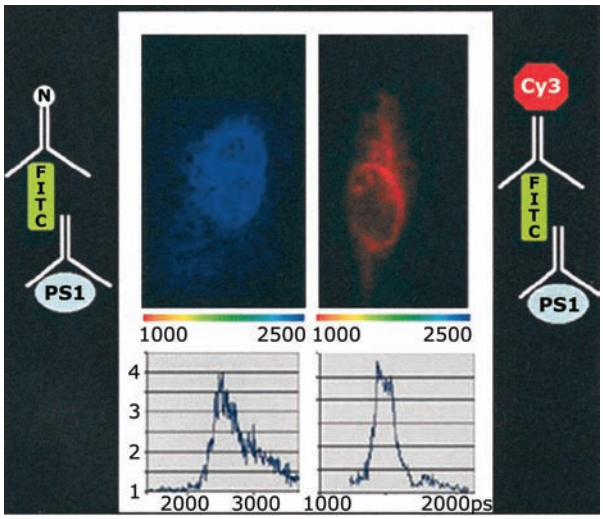

Figure 22.16. TCSPC lifetime images of CHO cells that express presenilin 1. The cell on the left was exposed to FITC-labeled antibody that bound near PS1. The cell on the right contained both FITC and Cy3-labeled antibodies near PS1. Revised from [53].

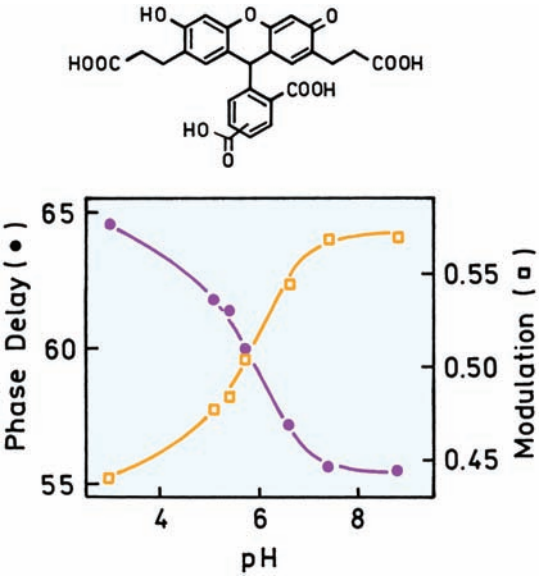

Figure 22.17. pH-dependent phase and modulation values of BCECF for 820 nm excitation with a Ti:sapphire laser, 80 MHz. Revised from [57].

except that the phase and modulation of the emission is measured rather than using TCSPC. An example of such measurements is lifetime imaging of the stratum corneum, which is the outermost layer of the skin. The lifetime probe was BCECF,[57] which displays a pH-dependent change in lifetime. This change was used to obtain a calibration curve of phase and modulation versus pH (Figure 22.17). The stratum corneum was imaged using two-photon excitation of BCECF at 820 nm. It was possible to obtain images at various depths in the stratum corneum because the long wavelength used for two-photon excitation can penetrate tissues and two-photon excitation is intrinsically confocal due to localized excitation at the focal point of the laser. The images of BCECF at a depth of 6.8 microns in the stratum corneum are shown in Figure 22.18. The intensity image shows that BCECF is present in the cells and in the interstitial spaces. The modulation is higher and the lifetime is lower in the interstitial spaces. These data allow the pH to be imaged within and around the keratinocytes. This result shows the ability of FLIM to provide quantitative molecular imaging using minimal perturbation of tissues.

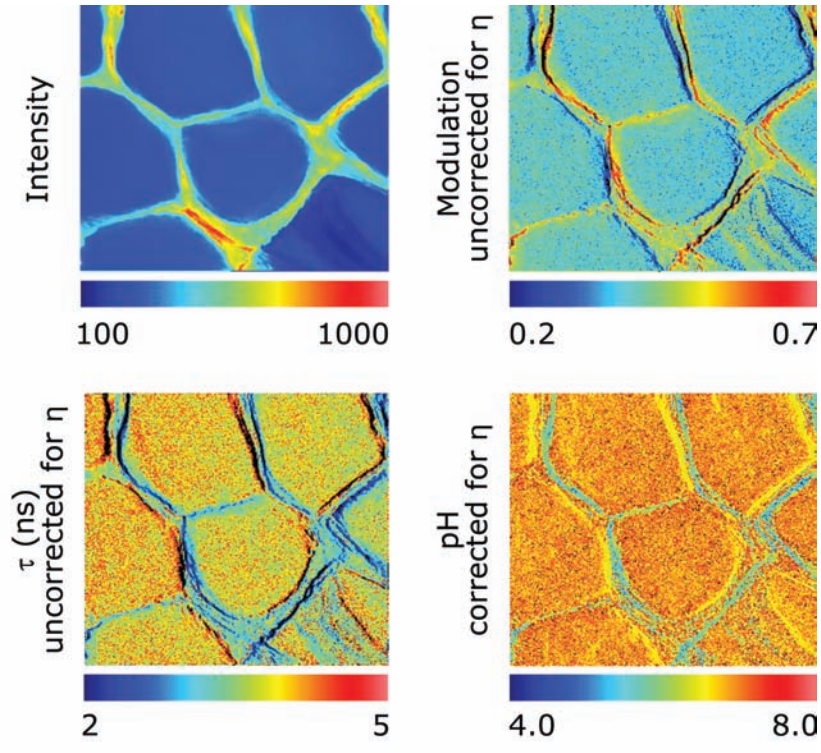

Figure 22.18. pH lifetime imaging of the skin stratum corneum at a depth of 6.8 microns using BCECF. See Figure 22.17. η is refractive index of the surrounding environment. Reprinted with permission from [57]. Images courtesy of Dr. Kerry M. Hanson from the University of Illinois at Urbana-Champaign.

22.7. CONCLUSIONS

FLIM is a robust method for molecular imaging that can be accomplished using several approaches, some of which are listed in the section entitled Additional Reading on Fluorescence-Lifetime Imaging Microscopy near the end of this chapter. FLIM can be used for imaging of ions, biomolecule proximity, and conditions that result in a change in the lifetime of the fluorophore. The instrumentation of FLIM is becoming simpler and less expensive, and can be created using modest modifications of existing instruments. The use of FLIM and the range of its applications is likely to expand greatly with the near future.

REFERENCES

1. Lakowicz JR, Berndt KW. 1991. Lifetime-selective fluorescence imaging using an rf phase-sensitive camera. *Rev Sci Instrum* **62**(7): 1727–1734.
2. Lakowicz JR, Szmacinski H, Nowaczyk K, Berndt BW, Johnson ML. 1992. Fluorescence lifetime imaging. *Anal Biochem* **202**:316–330.
3. Szmacinski H, Lakowicz JR, Johnson ML. 1994. Fluorescence lifetime imaging microscopy: homodyne technique using high-speed gated image intensifier. *Methods Enzymol* **240**:723–748.
4. Lakowicz JR, Szmacinski H, Nowaczyk K, Berndt KW, Johnson ML. 1993. Fluorescence lifetime imaging and application to Ca^{2+} imaging. In *Fluorescence spectroscopy: new methods and applications*, chap. 10. Ed OS Wolfbeis. Springer-Verlag, New York.
5. Veselova TV, Cherkasov AS, Shirokov VI. 1970. Fluorometric method for individual recording of spectra in systems containing two types of luminescent centers. *Opt Spectrosc* **29**:617–618.
6. Lakowicz JR, Szmacinski H, Nowaczyk K, Johnson ML, 1992. Fluorescence lifetime imaging of calcium using Quin-2. *Cell Calcium* **13**:131–147.
7. Lakowicz JR, Szmacinski H, Nowaczyk K, Johnson ML. 1994. Fluorescence lifetime imaging of intracellular calcium in COS cells using Quin-2. *Cell Calcium* **15**:7–27.
8. Gerritsen H, Draaijer A, Lakowicz JR. 1997. Introduction, second international lifetime imaging meeting, Utrecht, the Netherlands, June 14, 1996. *J Fluoresc* **7**(1):1–98.
9. Draaijer A, Sanders R, Gerritsen HC. 1995. Fluorescence lifetime imaging, a new tool in confocal microscopy. In *Handbook of biological confocal microscopy*, pp. 491–505. Ed JB Pawley. Plenum Press, New York.
10. Herman B, Wang XF, Wodnicki P, Perisamy A, Mahajan N, Berry G, Gordon G. 1999. Fluorescence lifetime imaging microscopy. In *Applied fluorescence in chemistry, biology and medicine*, pp. 491–507. Ed W Rettig, B Strehmel, S Schrader, H Seifert. Springer, Berlin.
11. Clegg RM, Holub O, Gohlke C. 2003. Fluorescence lifetime-resolved imaging: measuring lifetimes in an image. *Methods Enzymol* **360**:509–542.
12. Centonze VE, Sun M, Masuda A, Gerritsen H, Herman B. 2003. *Methods Enzymol* **360**:542–560.
13. Chen Y, Mills JD, Periasamy A. 2003. Protein localization in living cells and tissues using FRET and FLIM. *Differentiation* **71**:528–541.
14. Gadella TWJ, Jovin TM, Clegg RM. 1993. Fluorescence lifetime imaging microscopy (FLIM): spatial resolution of microstructures on the nanosecond time scale. *Biophys Chem* **48**:221–239.
15. Gadella TWJ, van Hoek A, Visser AJWG. 1997. Construction and characterization of a frequency-domain fluorescence lifetime imaging microscopy system. *J Fluoresc* **7**(1):35–43.
16. Birmingham JJ. 1997. Frequency-domain lifetime imaging methods at unilever research. *J Fluoresc* **7**(1):45–54.
17. Squire A, Verveer PJ, Bastiaens PIH. 2000. Multiple frequency fluorescence lifetime imaging microscopy. *J Microsc* **197**(pt.2):136–149.
18. Clayton AHA, Hanley QS, Arndt-Jovin DJ, Subramaniam V, Jovin TM. 2002. Dynamic fluorescence anisotropy imaging microscopy in the frequency domain (rFLIM). *Biophys J* **83**(3):1631–1649.
19. Clegg RM, Feddersen B, Gratton E, Jovin TM. 1992. Time-resolved imaging fluorescence microscopy. *Proc SPIE* **1640**:448–460.
20. Wouters FS, Bastiaens PIH. 1999. Fluorescence lifetime imaging of receptor tyrosine kinase activity in cells. *Curr Biol* **9**:1127–1130.
21. Verveer PJ, Squire A, Bastiaens PIH. 2001. Improved spatial discrimination of protein reaction states in cells by global analysis and deconvolution of fluorescence lifetime imaging microscopy data. *J Microsc* **202**(3):451–456.
22. Bastiaens PIH, Squire A. 1999. Fluorescence lifetime imaging microscopy: spatial resolution of biochemical processes in the cell. *Trends Cell Biol* **9**:48–52.
23. Pepperkok R, Squire A, Geley S, Bastiaens PIH. 1999. Simultaneous detection of multiple green fluorescent proteins in live cells by fluorescence lifetime imaging microscopy. *Curr Biol* **9**:269–272.
24. Dowling K, Hyde SCW, Dainty JC, French PMW, Hares JD. 1997. 2-D fluorescence lifetime imaging using a time-gated image intensifier. *Opt Commun* **135**:27–31.
25. Oida T, Sako Y, Kusumi A. 1993. Fluorescence lifetime imaging microscopy (flimscopy). *Biophys J* **64**:676–685.
26. Schneckenburger H, Konig K, Dienersberger T, Hahn R. 1994. Time-gated microscopic imaging and spectroscopy in medical diagnosis and photobiology. *Opt Eng* **33**(8):2600–2605.
27. Straub M, Hell SW. 1998. Fluorescence lifetime three-dimensional microscopy with picosecond precision using a multifocal multiphoton microscope. *Appl Phys Lett* **73**(13):1769–1771.
28. Elangovan M, Day RN, Periasamy A. 2002. Nanosecond fluorescence resonance energy transfer-fluorescence lifetime imaging microscopy to localize the protein interactions in a single living cell. *J Microsc* **205**(1):3–14.
29. Sharman KK, Periasamy A, Ashworth H, Demas JN, Snow NH. 1999. Error analysis of the rapid lifetime determination method for double-exponential decays and new windowing schemes. *Anal Chem* **71**:947–952.
30. Vereb G, Jares-Erijman E, Selvin PR, Jovin TM. 1998. Temporally and spectrally resolved imaging microscopy of lanthanide chelates. *Biophys J* **74**:2210–2222.
31. Herman B, Wodnicki P, Kwon S, Periasamy A, Gordon GW, Mahajan N, Wang XF. 1997. Recent developments in monitoring cal-

cium and protein interactions in cells using fluorescence lifetime microscopy. *J Fluoresc* **7**(1):85–91.
32. Schneckenburger H, Gschwend MH, Strauss WSL, Sailer R, Steiner R. 1997. Time-gated microscopic energy transfer measurements for probing mitochondrial metabolism. *J Fluoresc* **7**(1):3–10.
33. Webb SED, Gu Y, Lévêque-Fort S, Siegel J, Cole MJ, Dowling K, Jones R, French PMW, Neil MAA, Juskaitis R, Sucharov LOD, Wilson T, Lever MJ. 2002. A wide-field time-domain fluorescence lifetime imaging microscopy with optical sectioning. *Rev Sci Instrum* **73**(4):1898–1907.
34. Dowling K, Dayel MJ, Hyde SCW, French PMW, Lever MJ, Hares JD, Dymoke-Bradshaw AKL. 1999. High resolution time-domain fluorescence lifetime imaging for biomedical applications. *J Mod Opt* **46**(2):199–209.
35. Cole MJ, Siegel J, Webb SED, Jones R, Dowling K, Dayel MJ, Parsons-Karavassilis D, French PMW, Lever MJ, Sucharov LOD, Neil MAA, Juskaitis R, Wilson T. 2001. Time-domain whole-field fluorescence lifetime imaging with optical sectioning. *J Microsc* **203**(3):246–257.
36. Kentech Instruments Ltd., Oxfordshire, UK. http://www.kentech.co.uk.
37. LaVision Inc., Ypsilanti, Michigan. http://www.lavision.de/products/cameras/picostar/ picostar.htm.
38. Hamamatsu Corp. http://usa.hamamatsu.com.
39. Diaspro A. 2002. *Confocal and two-photon microscopy foundations, applications, and advances*. Wiley-Liss, New Jersey, 56.
40. Duncan RR, Bergmann A, Cousin MA, Apps DK, Shipston MJ. 2004. Multi-dimensional time-correlated single photon counting (TCSPC) fluorescence lifetime imaging microscopy (FLIM) to detect FRET in cells. *J Microsc* **215**(1):1–12.
41. Becker & Hickl GmbH, Berlin. http://www.becker-hickl.de.
42. Becker W, Hickl H, Zander C, Drexhage KH, Sauer M, Siebert S, Wolfrum J. 1999. Time-resolved detection and identification of single analyte molecules in microcapillaries by time-correlated single-photon counting (TCSPC). *Rev Sci Instrum* **70**(3):1835–1841.
43. Becker W, Bergmann A. 2004. Multi-dimensional time-correlated single photon counting. In *Review in fluorescence 2005*. Ed CD Geddes, JR Lakowicz. Springer, New York.
44. Becker W, Bergmann A, Hink MA, Konig K, Benndorf K, Biskup C. 2004. Fluorescence lifetime imaging by time-correlated single-photon counting. *Microsc Res Technol* **63**:58–66.
45. Becker W, Bergmann A, Weiss G. 2002. Lifetime imaging with the Zeiss LSM-510. *Proc. SPIE* **4620**:30–35.
46. Becker W, Bergmann A, Biscotti G, Koenig K, Riemann I, Kelbauskas L, Biskup C. 2004. High-speed FLIM data acquisition by time-correlated single photon counting. *Proc SPIE* **5323**:27–35
47. Becker W, Bergmann A, Biscotti G, Ruck A. 2004. Advanced time-correlated single photon counting technique for spectroscopy and imaging in biomedical systems. *Proc SPIE* **5340**:104–112
48. van der Oord CJR, de Grauw CJ, Gerritsen HC. 2001. Fluorescence lifetime imaging module LIMO for CLSM. *Proc SPIE* **4252**:119–123.
49. Becker W, Bergmann A. 2002. Multi-wavelength TCSPC lifetime imaging. *Proc SPIE* **4620**:79–84.
50. Becker W, Bergmann A, Konig K, Tirlapur U. 2001. Picosecond fluorescence lifetime microscopy by TCSPC imaging. *Proc SPIE* **4262**:414–419.
51. Köllner M, Wolfrum J. 1992. How many photons are necessary for fluorescence-lifetime measurements? *Chem Phys Lett* **200**:199–204.
52. Becker & Hickl GmbH, Berlin, Germany, http://www.becker-hickl.de, 2000. TCSPC adds a new dimension to 3D laser scanning microscopy. *Photonik* **3**:16–19
53. Berezovska O, Ramdya P, Skich J, Wolfe MS, Bacskai BJ, Hyman BT. 2003. Amyloid precursor protein associates with a nicastrin-dependent docking site on the presenilin 1-γ-secretase complex in cells demonstrated by fluorescence lifetime imaging. *J Neurosci* **23**(11):4560–4566.
54. Carlsson K, Liljeborg A. 1998. Simultaneous confocal lifetime imaging of multiple fluorophores using the intensity-modulated multiple-wavelength scanning (IMS) technique. *J Microsc* **191**(pt.2):119–127.
55. Gratton E, Breusegem S, Sutin J, Ruan Q, Barry N. 2003. Fluorescence lifetime imaging for the two-photon microscope: time-domain and frequency-domain methods. *J Biomed Opt* **8**(3):381–390.
56. Carlsson K, Liljeborg A, Andersson RM, Brismar H. 2000. Confocal pH imaging of microscopic specimens using fluorescence lifetimes and phase fluorometry: influence of parameter choice on system performance. *J Microsc* **119**(pt.2):106–114.
57. Hanson KM, Behne MJ, Barry NP, Mauro TM, Gratton E, Clegg RM. 2002. Two photon fluorescence lifetime imaging of the skin stratum corneum pH gradient. *Biophys J* **83**:1682–1690.
58. Molecular Probes product information FluoCels #1. http://www.probes.com/ servlets/product?item-14780.

ADDITIONAL READING ON FLUORESCENCE-LIFETIME IMAGING MICROSCOPY

Applications of FLIM

Calleja V, Ameer-Beg SM, Vojnovic B, Woscholski R, Downward J, Larijani B. 2003. Monitoring conformational changes of proteins in cells by fluorescence lifetime imaging microscopy. *Biochem J* **372**:33–40.

Eliceiri KW, Fan C-H, Lyons GE, White JG. 2003. Analysis of histology specimens using lifetime multiphoton microscopy. *J Biomed Opt* **8**(3):376–380.

Harpur AG, Wouters FS, Bastiaens PIH. 2001. Imaging FRET between spectrally similar GFP molecules in single cells. *Biotechnology* **19**: 167–169.

Marriott G, Clegg RM, Arndt-Jovin DJ, Jovin TM. 1991. Time resolved imaging microscopy, phosphorescence and delayed fluorescence imaging. *Biophys J* **60**:1374–1387.

Tadrous PJ, Siegel J, French PMW, Shousha S, Lalani E-N, Stamp GWH. 2003. Fluorescence lifetime imaging of unstained tissues: early results in human breast cancer. *J Pathol* **199**:309–317.

van Zandvoort MAMJ, de Grauw CJ, Gerritsen HC, Broers JLV, oude Egbrink MGA, Ramaekers FCS, Slaaf DW. 2002. Discrimination of DNA and RNA in cells by a vital fluorescent probe: lifetime imaging of SYTO13 in healthy and apoptotic cells. *Cytometry* **47**:226–235.

Vermeer JEM, Van Munster EB, Vischer NO, Gadella TWJ. 2004. Probing plasma membrane microdomains in cowpea protoplasts using lipidated GFP-fusion proteins and multimode FRET microscopy. *J Microsc* **214**(2):190–200.

Frequency-Domain FLIM

Clayton AHA, Hanley QS, Verveer PJ. 2004. Graphical representation and multicomponent analysis of single-frequency fluorescence lifetime imaging microscopy data. *J Microsc* **213**(1):1–5.

Gadella TWJ, van Hoek A, Visser AJWG. 1997. Construction and characterization of a frequency-domain fluorescence lifetime imaging microscopy system. *J Fluoresc* **7**(1):35–43.

Schneider PC, Clegg RM. 1997. Rapid acquisition, analysis, and display of fluorescence lifetime-resolved images for real-time applications. *Rev Sci Instrum* **68**(11):4107–4119.

Squire A, Bastiaens PIH. 1998. Three-dimensional image restoration in fluorescence lifetime imaging microscopy. *J Microsc* **193**(1):36–49.

Van Munster EB, Gadella TWJ. 2004. ϕFLIM: a new method to avoid aliasing in frequency-domain fluorescence lifetime imaging microscopy. *J Microsc* **213**(1):29–38.

Verveer PJ, Squire A, Bastiaens PIH. 2000. Global analysis of fluorescence lifetime imaging microscopy data. *Biophys J* **78**:2127–2137.

Wagnieres G, Mizeret J, Studzinski A, van den Bergh H. 1997. Frequency-domain fluorescence lifetime imaging for endoscopic clinical cancer photodetection: apparatus design and preliminary results. *J Fluoresc* **7**(1):75–83.

Gated CCD FLIM

Hartmann P, Ziegler W. 1996. Lifetime imaging of luminescent oxygen sensors based on all-solid-state technology. *Anal Chem* **68**:4512–4514.

Mitchell AC, Wall JE, Murray JG, Morgan CG. 2002. Direct modulation of the effective sensitivity of a CCD detector: a new approach to time-resolved fluorescence imaging. *J Microsc* **206**(3):225–232.

Mitchell AC, Wall JE, Murray JG, Morgan CG. 2002. Measurement of nanosecond time-resolved fluorescence with a directly gated interline CCD camera. *J Microsc* **206**(3):233–238.

Morgan CG, Mitchell AC, Murray JG, Wall EJ. 1997. New approaches to lifetime-resolved luminescence imaging. *J Fluoresc*. **7**(1):65–73.

Novel FLIM Methods

Dong CY, So PTC, French T, Gratton E. 1995. Fluorescence lifetime imaging by asynchronous pump-probe microscopy. *Biophys J* **69**:2234–2242.

Oxygen Imaging

Gerritsen HC, Sanders R, Draaijer A, Ince C, Levine YK. 1997. Fluorescence lifetime imaging of oxygen in living cells. *J Fluoresc* **7**(1):11–15.

Holst G, Franke U, Grunwald B. 2002. Transparent oxygen optodes in environmental applications at fine scale as measured by luminescence lifetime imaging. *Proc SPIE* **4576**:138–148.

Vinogradov SA, Lo L-W, Jenkins WT, Evans SM, Koch C, Wilson DF. 1996. Noninvasive imaging of the distribution in oxygen in tissue in vivo using near-infrared phosphors. *Biophys J* **70**:1609–1617.

pH Imaging

Lin H-J, Herman P, Lakowicz JR. 2003. Fluorescence lifetime-resolved pH imaging of living cells. *Cytometry* **52A**:77–89.

Sanders R, Draaijer A, Gerritsen HC, Houpt PM, Levine YK. 1995. Quantitative pH imaging in cells using confocal fluorescence lifetime imaging microscopy. *Anal Biochem* **227**:302–308.

Position Sensitive Detection

Charbonneau S, Allard LB, Young JF, Dyck YG, Kyle BJ. 1992. Two-dimensional time-resolved imaging with 100-ps resolution using a resistive anode photomultiplier tube. *Rev Sci Instrum* **63**(11):5315–5319.

Emiliani V, Sanvitto D, Tramier M, Piolot T, Petrasek Z, Kemnitz K, Durieux C, Coppey-Moisan M. 2003. Low-intensity two-dimensional imaging of fluorescence lifetimes in living cells. *Appl Phys Lett* **83**(12):2471–2473.

Kemnitz K, Pfeifer L, Paul R, Coppey-Moisan M. 1997. Novel detectors for fluorescence lifetime imaging on the picosecond time scale. *J Fluoresc* **7**(1):93–98.

Suhling K, Hungerford G, Airey RW, Morgan BL. 2001. A position-sensitive photon event counting detector applied to fluorescence imaging of dyes in sol-gel matrices. *Meas Sci Technol* **12**:131–141.

Tramier M, Gautier I, Piolot T, Ravalet S, Kemnitz K, Coppey J, Durieux C, Mignotte V, Coppey-Moisan M. 2002. Picosecond-hetero-FRET microscopy to probe protein–protein interactions in live cells. *Biophys J* **83**:3570–3577.

Reviews

Cubeddu R, Comelli D, D'Andrea C, Taroni P, Valentini G. 2002. Time-resolved fluorescence imaging in biology and medicine. *J Phys D: Appl Phys* **35**:R61–R76.

Gratton E, vandeVen MJ. 1995. Laser sources for confocal microscopy. In *Handbook of biological confocal microscopy*, pp. 61–97. Ed JB Pawley. Plenum Press, New York.

Periasamy A, Wang XF, Wodnick P, Gordon GW. 1995. High-speed fluorescence microscopy: lifetime imaging in the biomedical sciences. *J Microsc Soc Am* **1**(1):13–23.

Wang XF, Periasamy A, Wodnicki P, Gordon GW, Herman B. 1996. Time-resolved fluorescence lifetime imaging microscopy: instrumentation and biomedical applications. In *Fluorescence imaging spectroscopy and microscopy*, Chemical Analysis Series, Vol. 137, pp. 313–350. Ed XF Wang, B Herman. John Wiley & Sons, New York.

Streak Camera FLIM

Krishnan RV, Saitoh H, Terada H, Centonze VE, Herman B. 2003. Development of a multiphoton fluorescence lifetime imaging microscopy system using a streak camera. *Rev Sci Instrum* **74**(5):2714–2721.

Krishnan RV, Masuda A, Centonze VE, Herman B. 2003. Quantitative imaging of protein-protein interactions by multiphoton fluorescence lifetime imaging microscopy using a streak camera. *J Biomed Opt* **8**(3):362–367.

TCSPC FLIM

Ameer-Beg SM, Barber PR, Hodgkiss RJ, Locke RJ, Newman RG, Tozer GM, Vojnovic B, Wilson J. 2002. Application of multiphoton steady

state and lifetime imaging to mapping of tumor vascular architecture *in vivo*. *Proc SPIE* **4620**:85–95.

Biskup C, Kelbauskas L, Zimmer T, Benndorf K, Bergmann A, Becker W, Ruppersberg JP, Stockklausner C, Klocker N. 2004. Interaction of PSD-95 with potassium channels visualized by fluorescence lifetime-based resonance energy transfer imaging. *J Biomed Opt* **9**(4): 753–759.

Eliceiri KW, Fan C-H, Lyons GE, White JG. 2003. Analysis of histology specimens using lifetime multiphoton microscopy. *J Biomed Opt* **8**(3):376–380.

Jakobs S, Subramaniam V, Schonle A, Jovin TM, Hell SW. 2000. EGFP and DsRed expressing cultures of *Escherichia coli* imaged by confocal, two-photon and fluorescence lifetime microscopy. *FEBS Lett* **479**:131–135.

Konig K, Riemann I. 2003. High-resolution multiphoton tomography of human skin with subcellular spatial resolution and picosecond time resolution. *J Biomed Opt* **8**(3):432–439.

Theory

Carlsson K, Philip J. 2002. Theoretical investigation of the signal-to-noise ratio for different fluorescence lifetime imaging techniques. *Proc SPIE* **4622**: 70–73.

Hanley QS, Subramaniam V, Arndt-Jovin DJ, Jovin TM. 2001. Fluorescence lifetime imaging: multi-point calibration, minimum resolvable differences, and artifact suppression. *Cytometry* **43**:248–260.

Philip J, Carlsson K. 2003. Theoretical investigation of the signal-to-noise ratio in fluorescence lifetime imaging. *J Opt Soc Am A* **20**(2): 368–379.

Soloviev VY, Wilson DF, Vinogradov SA. 2004. Phosphorescence lifetime imaging in turbid media: the inverse problem and experimental image reconstruction. *Appl Opt* **43**(3):564–574.

Time-Gated FLIM

De Grauw CJ, Gerritsen HC. 2001. Multiple time-gated module for fluorescence lifetime imaging. *Appl Spectrosc* **55**(6):670–678.

Gerritsen HC, Asselbergs MAH, Agronskaia AV, Van Sark WGJHM. 2002. Fluorescence lifetime imaging scanning microscopes: acquisition speed, photon economy and lifetime resolution. *J Microsc* **206**(3):218–224.

Sytsma J, Vroom JM, De Grauw CJ, Gerritsen HC. 1998. Time-gated fluorescence lifetime imaging and microvolume spectroscopy using two-photon excitation. *J Microsc* **191**(1):39–51.

PROBLEMS

P22.1. Figures 22.15 and 22.19 show images of the same type of cells stained with the same three fluorophores. Explain the different colors of the images. Do the legends correctly identify each fluorophore?

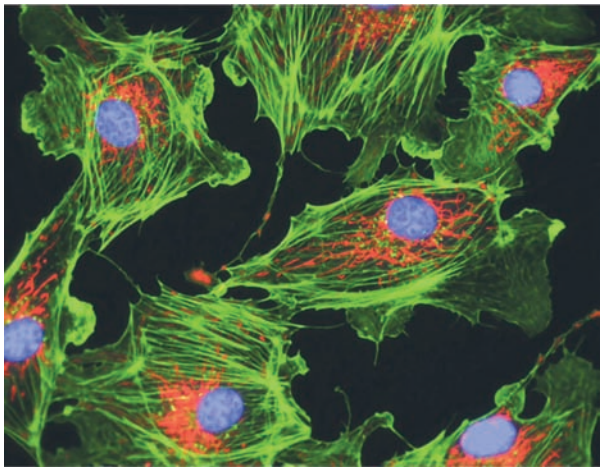

Figure 22.19. Fluorescence intensity images of bovine pulmonary artery endothelial cells stained with DAPI, Bodipy FL-phallacidin, and MitoTracker Red CMXRos. Multi-exposure image obtained with DAPI, fluorescein, and Texas Red filter sets. From [58].